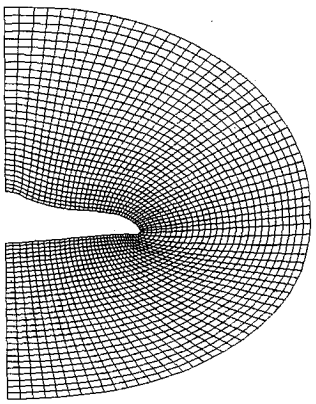

Fig. 2 Sectional grid with constant boundary spacing.

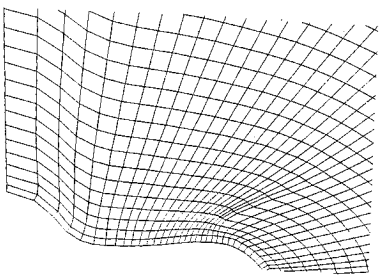

Fig. 3 Enlarged view of orthogonal sectional grid.

where

$$E = 1 - \eta^m \tag{6}$$

The subscripts i and o denote the inner and outer boundaries, respectively. Here, E plays a role analogous to that of a homotopy parameter. Modifications of E, therefore, cause slight deformations of a given map and may be used to achieve orthogonality and prescribed spacing at the inner boundary. This control is provided here through the use of the exponents p and q. These exponents are not constants with respect to τ and their values must be determined from the boundary data subject to the constraints of orthogonality and required spacing.

The orthogonality condition requires that the vectors A and B in Fig. 1 be orthogonal. The vector A is found by connecting the point (x_i,y_i) on the inner boundary and the point (x,y) lying just off the boundary on the trajectory in question. The second vector B passes through the point (x_i,y_i) and a point $(x,'y')$ on the line passing through (x_i,y_i) and parallel to the line joining (x_{i+1},y_{i+1}) and (x_{i-1},y_{i-1}) on the inner boundary. The orthogonality condition is that the dot product of the vectors A and B be zero, i.e.,

$$A \cdot B = 0 \tag{7}$$

which translates to

$$(x-x_i)(x'-x_i) + (y-y_i)(y'-y_i) = 0 \tag{8}$$

Substituting Eqs. (5) into Eq. (8), one obtains

$$(x_o-x_i)(1-E^p)(x'-x_i) + (y_o-y_i)(1-E^q)(y'-y_i) \tag{9}$$

The second condition, that of specified spacing ds in Fig. 1, can be written as

$$(x-x_i)^2 + (y-y_i)^2 = ds^2 \tag{10}$$

Substitution of Eqs. (5) into Eq. (10) results in

$$[(x_o-x_i)(1-E^p)]^2 + [(y_o-y_i)(1-E^q)]^2 = ds^2 \tag{11}$$

The exponents p and q can be solved for from Eqs. (9) and (11) and are found to be given by

$$p = \frac{\ell n\{1 + [B(y'-y_i)/(x_o-x_i)(x'-x_i)]\}}{\ell nE} \tag{12}$$

$$q = \frac{\ell n\{1 - [B/(y_o-y_i)]}{\ell n\, E} \tag{13}$$

where

$$B = \frac{ds}{\sqrt{1 + [(y'-y_i)^2/(x'-x_i)^2]}} \tag{14}$$

and E has the value corresponding to the homotopic curve lying next to the inner boundary.

Results and Discussions

A planar grid presented in Fig. 2 shows that the grid spacing adjacent to the inner boundary is constant along the circumference. The grid is also seen to be smooth, orthogonal at the inner boundary, and free from intersecting trajectories. It may be noticed in the grid presented in Fig. 3 that, although nearly orthogonal and nonintersecting grids can be generated by the present code, complex boundary shapes may cause local nonuniformities in the grid. In such complex cases, the algebraic grid produced by the present method may be postprocessed by an elliptic smoother.

References

[1]Moitra, A., "Quasi-Three-Dimensional Grid Generation by an Algebraic Homotopy Procedure," *Numerical Grid Generation in Computational Fluid Mechanics '88*, Pineridge, Swansea, Wales, UK.

[2]Moitra, A., "Numerical Solution of the Euler Equations for High-Speed, Blended Wing-Body Configurations," AIAA Paper 85-0123, Jan. 1985.

[3]Moitra, A., "Euler Solutions for High-Speed Flow About Complex Three-Dimensional Configurations," AIAA Paper 86-0246, Jan. 1986.

Efficiency of a Statistical Transport Model for Turbulent Particle Dispersion

Ron J. Litchford* and San-Mou Jeng†
University of Tennessee Space Institute, Tullahoma, Tennessee 37388

Introduction

A STATISTICAL transport model for turbulent particle dispersion was recently introduced in this journal[1] having significant potential for improving the computational efficiency and robustness of spray combustion CFD analyses. The technique was based on coupling a stochastic direct-modeling approach for parcel/eddy interaction properties with continuous probability density functions (pdf) to describe the physical particle temporal and spatial distribution. More specif-

Received March 21, 1991; revision received Aug. 6, 1991; accepted for publication Aug. 12, 1991.

*Research Engineer, UT-Calspan Center for Advanced Space Propulsion. Member AIAA.

†Assistant Professor, Mechanical and Aerospace Engineering; currently, Associate Professor, Aerospace Engineering and Engineering Mechanics, Univ. of Cincinnati, Cincinnati, OH 45221. Member AIAA.

ically, a computational parcel representing a group of physical particles is characterized by a normal (Gaussian) pdf in space. The mean of each pdf is determined by Lagrangian tracking of a computational parcel through a sequence of stochastically generated turbulent eddies. The variance of each pdf is represented by a turbulence-induced mean-square dispersion based on a statistical formulation of the linearized particle equations of motion. This technique provides for reduced sampling requirements with minimal computational shot noise and was shown to produce good time-averaged dispersion results in comparison to the conventional direct-modeling approach.

In developing the theoretical formulation for turbulent dispersion transport, however, a generalized approach was taken such that the perturbing influence of each turbulent eddy on following interactions was transported through all subsequent eddies. In fact, a close examination of the formulated transport relation reveals that this perturbing influence can decay rapidly. Thus, additional computational efficiency may be obtained by truncation of unnecessary transport terms. This Note addresses the criterion for truncation and expected gains in efficiency.

Theoretical

The fundamental statistical relation formulated for turbulent particle dispersion transport derives from a linear combination of fully uncorrelated turbulent velocity fluctuations as an expression for the variance of the parcel pdf after the nth interaction[1]:

$$\sigma_{p_n}^2 \approx \sum_{k=1}^{n} (u'_{g_{\mathrm{rms}_k}} T_k)^2 \tag{1}$$

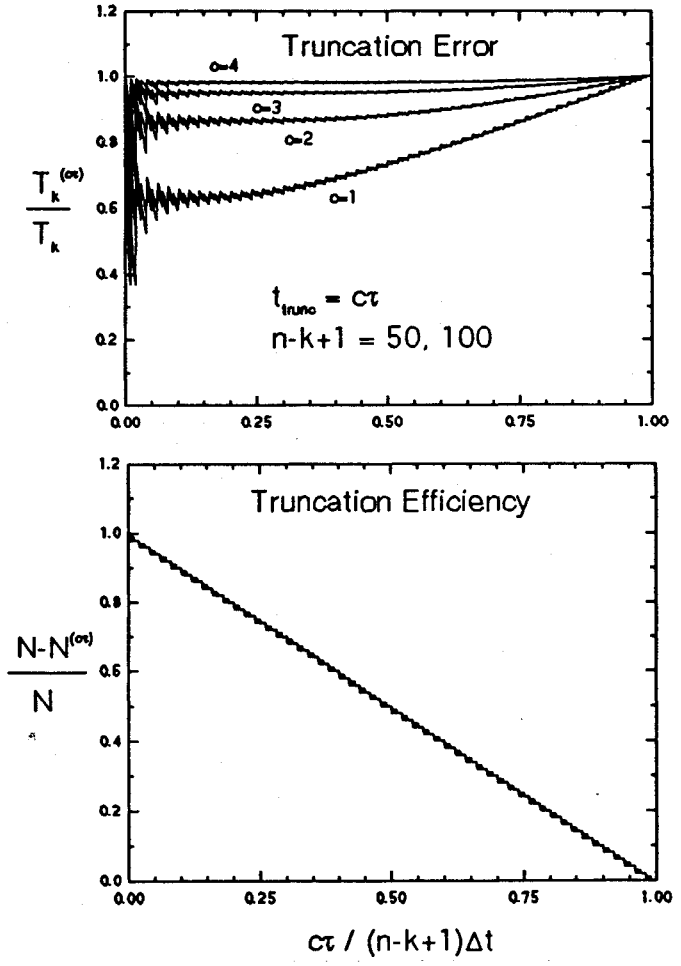

Fig. 1 Truncation error and efficiency as a function of $c\tau/(n-k+1)\Delta t$.

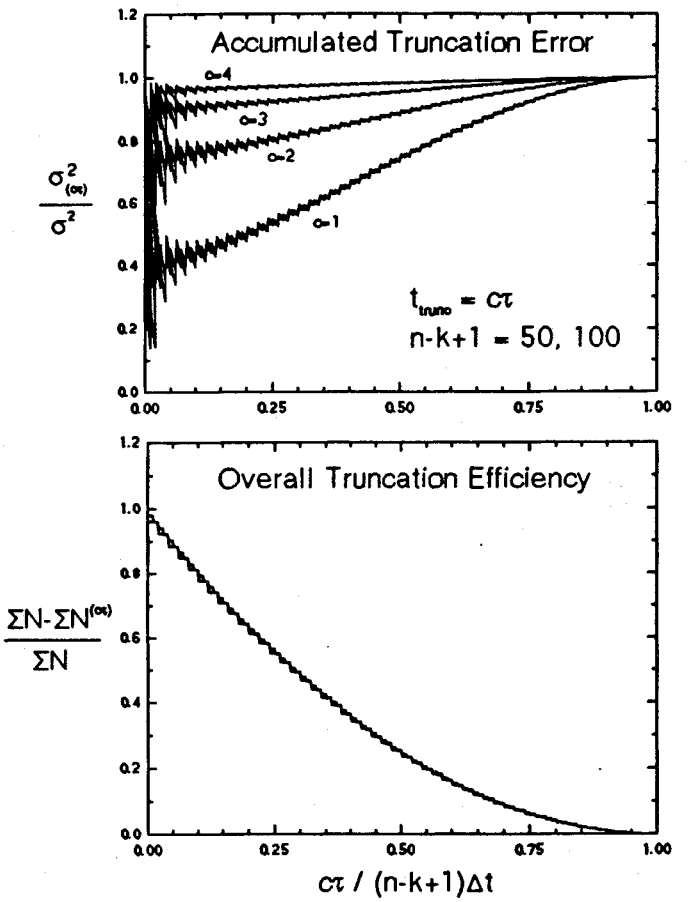

Fig. 2 Accumulated truncation error and overall truncation efficiency as a function of $c\tau/(n-k+1)\Delta t$.

where $u'_{g_{\mathrm{rms}_k}}$ is the root-mean-square turbulent gas-phase velocity fluctuation in the kth eddy and T_k is the turbulent transport factor which essentially acts as an effective time constant for turbulent dispersion carrying the perturbing influence originating in the kth interaction through subsequent eddies leading to the nth interaction. The transport factor T_k was derived as a function of the interaction time Δt_i and the particle time constant τ_i in the form

$$T_k = (\Delta t_k - \tau_k A_k) + A_k \Bigg\{ \tau_{k+1} A_{k+1} + \tau_{k+2} A_{k+2} \exp\left[-\frac{\Delta t_{k+1}}{\tau_{k+1}} \right] + \tau_{k+3} A_{k+3} \exp\left[-\left(\frac{\Delta t_{k+1}}{\tau_{k+1}} + \frac{\Delta t_{k+2}}{\tau_{k+2}} \right) \right] + \cdots + \tau_n A_n \exp\left[-\left(\frac{\Delta t_{k+1}}{\tau_{k+1}} + \frac{\Delta t_{k+2}}{\tau_{k+2}} + \cdots + \frac{\Delta t_{n-1}}{\tau_{n-1}} \right) \right] \Bigg\} \tag{2}$$

where

$$A_l = 1 - \exp\left[\frac{-\Delta t_l}{\tau_l} \right]$$

The expression for T_k is essentially a summation over $(n-k+1)$ terms of the general form

$$T_k = f_k + f_{k+1} + f_{k+2} + \cdots + f_n \tag{3}$$

where f_k represents the dispersion directly induced by the originating kth eddy, f_{k+1} represents the dispersing influence of the kth eddy as transported to the first subsequent eddy, and so on to f_n which represents the dispersing influence of the kth eddy as transported to the nth eddy.

This general formulation for the turbulent dispersion transport factor T_k accounts for the propagation of the disturbing influence originating in the kth eddy through all interactions $k \rightarrow n$. Note also that T_k is evaluated for every interaction preceeding the nth eddy. While providing a complete and general description of the dispersing transport process, such a recursive formulation is computationally expensive and reduction in computing effort is sought. By inspection of the exponential operators in Eq. (2), it is clear that the terms in Eq. (3) may diminish rapidly suggesting a truncation criterion for the summation. Indeed, if we require that all τ_i approach zero, we find $\lim_{\tau_i \to 0} T_k \rightarrow \Delta t_k$ implying that only the first term in the summation need be retained. This behavior is physically interpreted as a particle having almost instantaneous dynamic response to a turbulent velocity fluctuation in an eddy such that no residual particle velocity fluctuation is transported into subsequent eddies. In the opposite extreme of infinitly large τ_i, a particle would have essentially no dynamic response to a turbulent velocity fluctuation and there would be no dispersing effect. In the practical realm of interest where τ will take on moderate values, however, we can expect that some residual particle velocity fluctuation will generally be transported beyond the originating kth eddy and that this effect will be washed out within some small number of subsequent interactions. Thus, a satisfactory truncation criterion whereby T_k need only be evaluated for eddies $k \rightarrow m$ where $m \leq n$ would be desirable in terms of computational efficiency.

To examine the characteristic errors and gains in efficiency one might expect using a time-based truncation criterion, a simple analysis is made where Δt and τ are restricted to have constant values for every interaction so that the analysis remains tractable. It is then possible to form the ratio $T_k^{(c\tau)}/T_k$ where T_k is evaluated for $k \rightarrow n$ interactions and $T_k^{(c\tau)}$ is evaluated for $k \rightarrow m$ interactions with m determined from the criterion

$$\sum_{i=k}^{m} \Delta t_i \geq c\tau \tag{4}$$

which for constant τ and Δt may be expressed in terms of the dimensionless time-scale ratio as

$$m - k + 1 \geq \frac{c}{\Delta t/\tau}$$

The truncation constant is specified by c, and $(m - k + 1)$ is the minimum number of interactions needed so that the amount of time allowed for transporting the influence of the kth eddy just exceeds the truncation time $c\tau$. The expression for $T_k^{(c\tau)}/T_k$, which characterizes the turbulent transport factor truncation error, takes the dimensionless form

$$\frac{T_k^{(c\tau)}}{T_k} = \frac{\left(1 - \frac{\tau A}{\Delta t}\right) + \frac{\tau A^2}{\Delta t}\left\{1 + \exp\left[-\frac{\Delta t}{\tau}\right] + \exp\left[-\frac{2\Delta t}{\tau}\right] + \cdots + \exp\left[-\frac{(m-k-1)\Delta t}{\tau}\right]\right\}}{\left(1 - \frac{\tau A}{\Delta t}\right) + \frac{\tau A^2}{\Delta t}\left\{1 + \exp\left[-\frac{\Delta t}{\tau}\right] + \exp\left[-\frac{2\Delta t}{\tau}\right] + \cdots + \exp\left[-\frac{(n-k-1)\Delta t}{\tau}\right]\right\}} \tag{5}$$

Since evaluation of dispersion for $(n - k + 1)$ interactions requires a summation of $(n - k + 1)$ terms involving a like number of transport factors, it is also useful to examine how the truncation errors associated with these transport factors accumulate to affect the accuracy in the pdf variance after the nth interaction. For simplicity, we consider here the special case where $u'_{g_{\text{rms}_k}}$ is taken as identical for every interaction so that the accumulated truncation error may be expressed by the dimensionless ratio

$$\sigma^2_{(c\tau)}/\sigma^2 = \sum_{k=1}^{n} (T_k^{(c\tau)})^2 \Big/ \sum_{k=1}^{n} (T_k)^2 \tag{6}$$

It is now possible to evaluate the characteristic truncation errors and gains in efficiency as a function of the time-scale ratio $\tau/\Delta t$ for various values of the truncation constant.

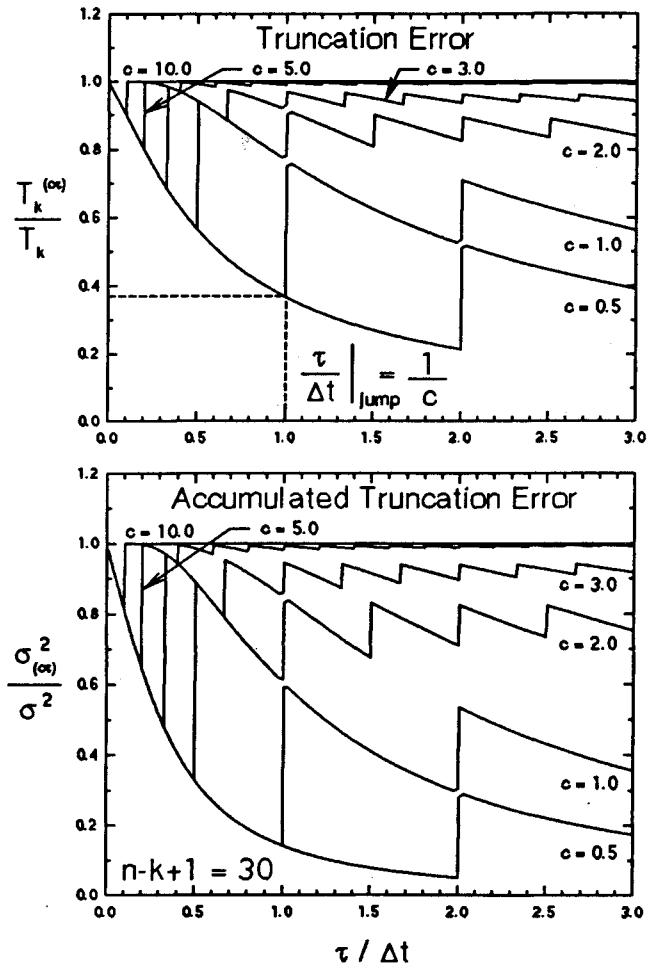

Fig. 3 Truncation errors as function of $\tau/\Delta t$.

Results

Evaluation of the transport factor truncation error was carried out by specifying a value for the truncation constant and computing $T_k^{(c\tau)}/T_k$ as a function of $\tau/\Delta t$ for an arbitrary number of interactions. These results were plotted with respect to the reduced time-scale ratio $c\tau/(n - k + 1)\Delta t$ (which is directly analogous to the ratio m/n in this simplified case) so that the behavior of the truncation error is described by a unique family of curves for each value of the truncation constant. Each curve within a family then corresponds to the number of interactions evaluated. This generalized description of the truncation error is depicted in Fig. 1 for 50 and 100 interaction evaluations with $c = 1, 2, 3, 4$. The truncation efficiency defined by the ratio $(N - N^{(c\tau)})/N$, where N represents the number of terms used in evaluating the turbulent transport factor, is also presented in Fig. 1 as a function of $c\tau/(n - k + 1)\Delta t$. The efficiency is found linearly dependent on the reduced time-scale ratio and independent of the value of the truncation constant.

For the constant property case considered, it is evident that the truncation error can become unacceptably large if the truncation constant is too small. Also observe the general oscillatory nature of the error which is a direct result of the

linearization approximation imposing finite time increments. The greatest error for a specified truncation constant is found to occur as $c\tau$ approaches Δt, although this is obscured by the overlapping of multiple curves in the figure. Note that when the truncation time $c\tau$ exceeds the total interaction time $(n - k + 1)\Delta t$, $m = n$ and no truncation is allowed. The truncation efficiency is seen to exceed 95% with diminishing $\tau/\Delta t$ and to vanish when the truncation time exceeds the total interaction time.

Evaluation of the accumulated truncation errors in the pdf variance as well as the associated overall truncation efficiency for various values of c are similarly shown in Fig. 2 as a function of $c\tau/(n - k + 1)\Delta t$. As expected, we find the same qualitative behavior where the accumulated truncation error becomes quite large for small values of the truncation constant. However, reduced error levels are still obtainable with moderately increased values of c. The overall truncation efficiency collapses to a characteristic parabolic profile for all values of the truncation constant and indicates that considerable savings in the overall computational effort is possible.

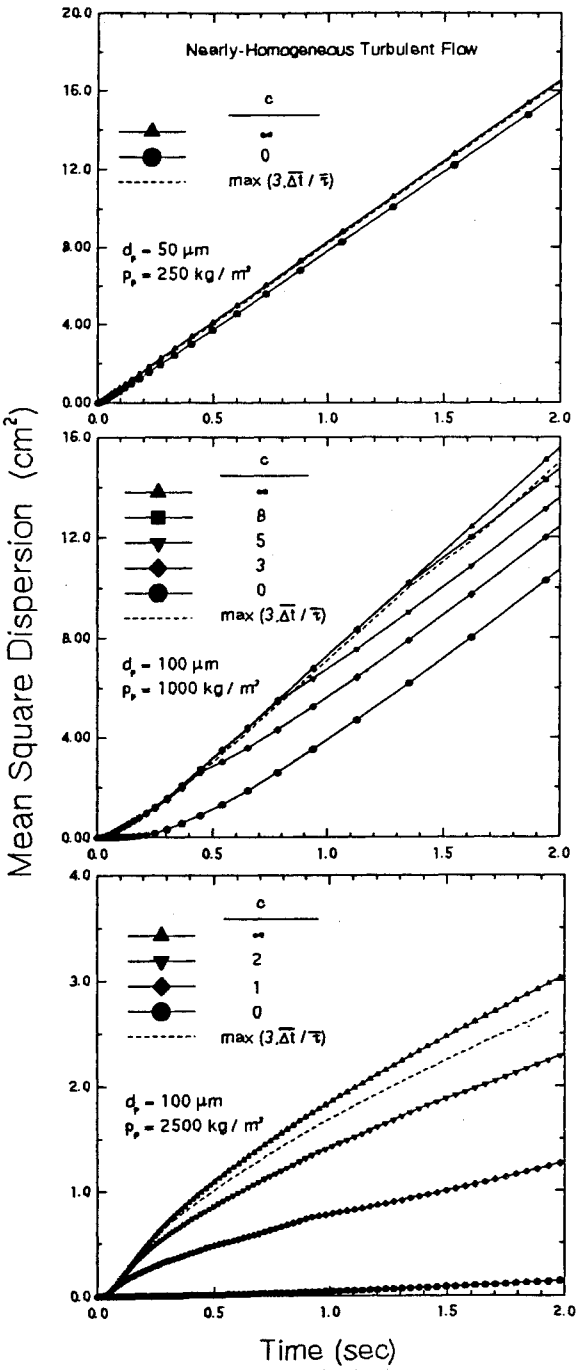

Fig. 4 Mean-square dispersion with time for various truncation criteria.

It would appear that the simple time-based truncation criterion of Eq. (4) with a moderate value for c is sufficient to insure a desired minimal truncation error as long as $c\tau \geq \Delta t$. This is demonstrated more succinctly in Fig. 3 which depicts the truncation errors directly as a function of $\tau/\Delta t$ for various imposed values of the truncation constant. We note here that some of the data have been purposely altered at the discontinuities to prevent the multiple curves from intersecting and obscuring discernment of each individual curve. In this plot, we observe that the error follows a unique characteristic exponential growth during well-defined intervals of $\tau/\Delta t$. The discontinuous jumps between these intervals occur whenever $c\tau$ is an integer multiple of Δt. This behavior is illustrated explicitly at the first multiple when $c = 1$ in Fig. 3. Clearly, the greatest error occurs just before the first multiple as $c\tau$ approaches Δt. It is also obvious that a modest increase in c cannot prevent undesirable errors in this regime. For example, the accumulated truncation error may reach 20% even when $c = 10$. To circumvent this difficulty, however, we can use our knowledge for locating the first multiple jump corresponding to a given value of c to construct an appropriate truncation criterion. For instance, a simple criterion capable of maintaining an acceptable maximal error limit with optimal efficiency would be to apply Eq. (4) with the truncation constant obtained as $\max(c_0, \Delta t/\tau)$ where c_0 is the nominal truncation constant appropriate for maintaining a set error limit when $c_0\tau \geq \Delta t$.

The analysis presented above is for seemingly quite restrictive conditions—constant Δt and τ. But the basic qualitative results have general applicability to the practical situation where the time-scale parameters vary throughout the flow. For practical sprays, it is necessary to obtain the truncation criterion more tentatively. By introducing a running average evaluation for the time-scale parameters, such a criterion might be established through the relation

$$\sum_{i=k}^{m} \Delta t_i \geq c\bar{\tau}, \qquad c = \max\left(c_0, \frac{\overline{\Delta t}}{\bar{\tau}}\right) \tag{7}$$

where $\bar{\tau}$ and $\overline{\Delta t}$ are running averages of τ_i and Δt_i, respectively, for all interactions $k \rightarrow m$ and c_0 is again the nominal truncation constant. An appropriate value of c_0 necessary to obtain a desired level of accuracy could be estimated based on the preceeding simplified analysis. Alternatively, it could be established more rudimentarily by randomly selecting parcels injected into the computational domain and evaluating the overall truncation error associated with a specified value of c_0. In fact, such an empirical validation procedure is essential in establishing the truncation criterion for various flow conditions.

To demonstrate, we validate the proposed truncation criterion here for rigid particles of various size and mass injected into a grid-generated nearly homogeneous turbulent flow as empirically described in the experimental work of Snyder and Lumley.[2] Particles were injected at the mean flow velocity and tracked through a sequence of stochastically generated turbulent eddies as described in our previous publication,[1] and the mean-square dispersion was computed from Eq. (1) based on the truncation criterion, Eq. (7), with $c_0 = 3$ and also with c constrained as an arbitrary constant. Results are presented in Fig. 4 indicating that the basic truncation criterion evolved from our simplified analysis may be successfully extended to the practical case. For the lightest and smallest particle considered ($d_p = 50$ μm; $\rho_p = 250$ kg/m^3), we find that only the first term in the summation for the transport factor is of any consequence. For the moderately sized particle considered ($d_p = 100$ μm; $\rho_p = 1000$ kg/m^3), it is evident that the perturbing influence of an eddy can propagate through a substan-

tial number of eddies before decaying and that the modification for the interval preceeding the first multiple jump in the criterion, Eq. (7), is important in preventing unacceptable errors. For the most massive particle considered ($d_p = 100\ \mu$m; $\rho_p = 2500$ kg/m^3), $c_0 > \Delta t/\bar{\tau}$ and $c = c_0$ for all interactions.

For practical application of the truncation criterion suggested in this technical note, it will certainly be necessary to first validate the criterion for the flow conditions of particular interest, as demonstrated herein for nearly homogeneous turbulent flow. Once established, however, the potential gains in efficiency, through elimination of unnecessary and redundant computational operations, may be significant.

Acknowledgments

This work was conducted as part of an ongoing spray combustion stability project supported by the University of Tennessee-Calspan Center for Advanced Space Propulsion, UT Space Institute, Tullahoma, TN under NASA Grant NAGW-1195 and in part by Rocketdyne Division, Rockwell International, Canoga Park, CA with Merlin Schuman as technical monitor.

References

[1]Litchford, R. J., and Jeng, S.-M., "Efficient Statistical Transport Model for Turbulent Particle Dispersion in Sprays," *AIAA Journal,* Sept. 1991, pp. 1443-1451.

[2]Snyder, W. H., and Lumley, J. L., "Some Measurements of Particle Velocity Autocorrelation Functions in a Turbulent Flow," *Journal of Fluid Mechanics,* Vol. 48, 1971, pp. 41-71.

Cylindrical Bending of Unsymmetric Composite Laminates

Hsin-Piao Chen*
California State University at Long Beach, Long Beach, California 90840
and
Jeffrey C. Shu†
The Aerospace Corporation, El Segundo, California 90245

Introduction

EARLY work on unsymmetric laminate analysis was mostly based on the linear classical lamination theory. Recently, Sun and Chin[1,2] found that the linear lamination theory is inadequate for analysis of unsymmetric laminates, and the nonlinear large deflection theory must be used even for problems that are normally considered to be in the small deflection domain. In their studies, however, the transverse shear effect was not considered. This effect is important for resin matrix composite laminates because the interlaminar shear moduli of composite materials are very small as compared with the in-plane elastic moduli of reinforced fiber. A recent study by Chen,[3] using a large deflection shear deformation theory on the delamination buckling, postbuckling, and growth behaviors of composite laminates, has demonstrated the importance of transverse shear effects for different delamination sizes.

This Note presents a solution for unsymmetric cross-ply laminates, including both large deflection and transverse shear effects. A pinned-pinned laminated plate subjected to a uniform transverse load is demonstrated. The results from the nonlinear shear deformation theory (NSDT) are also compared with those from the nonlinear classical lamination theory (NCLT),[1,2] the linear shear deformation theory (LSDT), and the linear classical lamination theory (LCLT).

Formulation

Consider an unsymmetric cross-ply laminate subjected to a uniform transverse load. For cylindrical bending, the governing equations are assumed to be independent of the y axis. Based on the large deflection shear deformation formulation,[3] the laminate displacements u and w are expressed by

$$u(x,z) = u^0(x) + z\psi_x(x) \tag{1}$$

$$w(x,z) = w(x) \tag{2}$$

where u^0 is the midplane displacement and ψ_x is the rotation in the xz plane. The equilibrium equations are given by

$$N_{x,x} = 0 \tag{3}$$

$$M_{x,x} - Q_x = 0 \tag{4}$$

$$Q_{x,x} + N_x w_{,xx} + q = 0 \tag{5}$$

where N_x, M_x, and Q_x are membrane force, bending moment, and transverse shear force resultants, respectively, and q is the transverse loading. The constitutive relations for the cross-ply laminates are characterized by

$$N_x = A_{11}(u^0_{,x} + \tfrac{1}{2}w^2_{,x}) + B_{11}\psi_{x,x} \tag{6}$$

$$M_x = B_{11}(u^0_{,x} + \tfrac{1}{2}w^2_{,x}) + D_{11}\psi_{x,x} \tag{7}$$

$$Q_x = kA_{55}(\psi_x + w_{,x}) \tag{8}$$

where A_{11}, D_{11}, B_{11}, and A_{55} are extensional, bending, extension-bending coupling, and transverse shear stiffnesses, respectively, and k is the shear correction factor.

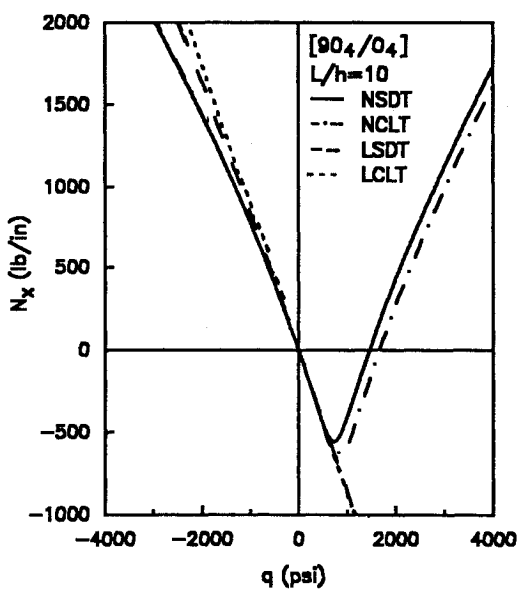

Fig. 1 In-plane force induced by transverse loading based on linear and nonlinear theories.

Presented as Paper 91-0961 at the AIAA/ASME/ASCE/AHS/ACS 32nd Structures, Structural Dynamics, and Materials Conference, Baltimore, MD, April 8-10, 1991; received May 9, 1991; revision received Aug. 13, 1991; accepted for publication Aug. 15, 1991.

*Associate Professor, Department of Aerospace Engineering. Member AIAA.

†Member of the Technical Staff.